

## Specific heat and magnetic susceptibility of nearly stoichiometric and homogeneous Nb<sub>3</sub>Al

A. Junod, J.-L. Jorda, M. Pelizzone, and J. Muller

*Département de Physique de la Matière Condensée, Université de Genève, CH-1211 Genève 4, Switzerland*

(Received 21 June 1983)

A15-type Nb<sub>3</sub>Al has been characterized in the recent past as a "high- $T_c$ , low- $\gamma$  superconductor," where  $\gamma$  is the electronic specific-heat coefficient. We show that this statement should be revised, previous analyses simply reflecting the imperfect metallurgical state. We succeeded in preparing homogeneous, nearly stoichiometric, bulk Nb<sub>3</sub>Al and reinvestigated the specific heat (from 1 to 50 K) and the magnetic susceptibility (19–300 K) in the highly ordered and a slightly disordered condition. The new results show that ordered Nb<sub>3</sub>Al exhibits a high electronic density of states ( $\gamma = 11.4 \text{ mJ K}^{-2} \text{ g-at.}^{-1}$ ,  $N(0) \cong 0.91 \text{ eV}^{-1} \text{ atom}^{-1} \text{ spin}^{-1}$ ). Information is provided on the moments of the phonon spectrum and those of the electron-phonon spectral function, the thermodynamical critical field, and the energy gap  $2\Delta(0)$ . The present experiments further establish only weak exchange enhancement of the susceptibility; spin fluctuations may therefore be safely neglected. Specific-heat data are also reported for the neighboring  $\sigma$ -phase Nb<sub>2</sub>Al.

### I. INTRODUCTION

The A15-phase compound Nb<sub>3</sub>Al is known to be superconducting at a temperature close to 18.8 K.<sup>1</sup> In fact, specific-heat measurements show that the superconducting transition is generally smeared over a fairly large temperature interval. This is due to a peculiarity of the Nb-Al phase diagram. If a sample with a nominal 3:1 composition is prepared from the melt, some segregation always occurs during cooling because the equilibrium composition of the A15 phase is not stoichiometric at room temperature. The resulting composition is then distributed from  $\approx 22$  to  $\approx 25$  at. % Al. It has been found experimentally, however, that this phenomenon can be largely avoided by fast-cooling methods and careful heat treatments.

In this article, we report new specific-heat and magnetic susceptibility measurements performed on nearly stoichiometric and homogeneous Nb<sub>3</sub>Al samples. The physical parameters found differ markedly from those accepted so far. The ordering effect obtained by annealing is also studied, and leads to an upper limit for spin-fluctuation effects. Finally, estimates of the microscopic physical parameters that govern superconductivity based on the heat-capacity data in the normal and the superconducting states will be given and compared with data from other sources.

### II. PREPARATION

The phase diagram of the Nb-Al system has been reexamined recently;<sup>2</sup> the implications on the superconductivity of the A15 phase have already been reported.<sup>3</sup> The A15 phase is formed from the Nb solid solution and the liquid by the peritectic reaction  $\text{Nb(s.s.)} + \text{liquid} \leftrightarrow \text{Nb}_{0.775}\text{Al}_{0.225}$  at  $2060 \pm 10^\circ\text{C}$ . The homogeneity range approaches the stoichiometric composition Nb<sub>0.75</sub>Al<sub>0.25</sub> at  $1940 \pm 10^\circ\text{C}$  when the peritectic reaction  $\text{Nb}_3\text{Al(A15)} + \text{liquid}$

$\leftrightarrow \text{Nb}_{0.68}\text{Al}_{0.32}$  ( $\sigma$  phase) sets in. Below this temperature, the stability limit shifts to lower Al contents and the A15-phase field extends only from 18.5 to 21 at. % Al at  $1000^\circ\text{C}$ ; however, equilibration times become exceedingly long below this temperature and no more segregation occurs when the sample is annealed at  $750^\circ\text{C}$ .

The sample under study (labeled 255cs) was prepared by arc-melting starting from 99.95%-pure Nb powder (Johnson Matthey) and Al rods (99.99% purity) from Balzers. The alloy was melted three times in order to ensure homogeneity; the weight losses supposedly due exclusively to Al vaporization were compensated by Al additions. The final uncertainty in composition was less than 0.5 at. %. The sample was then annealed for 63 h at  $1850^\circ\text{C}$  under 4 atm of Ar. From this master ingot small slices  $\approx 1.5$  mm thick were cut by spark erosion, submitted to a new high-temperature anneal (2 min at  $1940^\circ\text{C}$ ), and then rapidly cooled by an argon jet (cooling rate  $\approx 10^4$  K/s).

X-ray analysis using the Guinier technique with Cu  $K\alpha$  radiation showed no other phase than the A15 with a lattice constant  $a_0 = 5.180 \pm 0.001$  Å measured with Si as an internal standard. Referring to the phase diagram, this lattice parameter corresponds to  $25 \pm 0.5$  at. % Al in the alloy, i.e., the stoichiometric composition.

The microstructure of the sample was observed after polishing and etching with a  $\text{HNO}_3 + \text{H}_2\text{SO}_4 + \text{HF} + \text{H}_2\text{O}$  solution. As expected, a Widmannstätten-type pattern is observed, an experimental clue confirming the stoichiometric composition.

After the measurements in this "disordered" state had been completed, the sample was annealed for eight weeks at  $750^\circ\text{C}$  before new measurements were taken.

### III. SPECIFIC HEAT

The apparatus used in this study is a calorimeter of the quasiadiabatic type provided with a mechanical heat

switch. The temperature scale relies on primary thermometry: He vapor pressure and gas thermometer pressure measured by digital gauges. As a test of the reproducibility of the measurements (this will be of some importance in the discussion of ordering effects), a 870-mg copper sample (99.999% purity) was measured before and after the Nb<sub>3</sub>Al runs. The values found for  $\gamma$  were 0.694 and 0.696 mJ K<sup>-2</sup> g-at.<sup>-1</sup>, and for  $\Theta$ , 344 and 342 K. These data may be compared with the generally accepted values<sup>4</sup> of 0.695 mJ K<sup>-2</sup> g-at.<sup>-1</sup> and 344.5 K, respectively.

The 1.4-g sample of Nb<sub>3</sub>Al was glued to a sapphire sample holder with grease.<sup>5</sup> The total heat capacity of the addenda (1.23 g sapphire, 7 mg grease, and  $\approx$ 3 mg miscellaneous) was measured separately and found to be equal to the sum of the heat capacity of the constituents. The contribution of the addenda amounts typically to 23% of the total heat capacity at 1.3 K and falls to 10% at 10 and 40 K in the Nb<sub>3</sub>Al runs.

The data obtained between 1.3 and 50 K are presented in Fig. 1. The shape of the specific-heat jump at the superconducting transition temperature  $T_c$  is characteristic of a homogeneous sample. The curvatures of the normal-state data contain informations on the shape of the phonon spectrum. At the lower end of the temperature range (Fig. 2), the data in the superconducting state follow closely a law of the form  $C/T = \gamma_0 + \beta T^3$ . The absence of any curvature in this plot means that the contribution of the superconducting electrons is negligible below  $T_c/6$ , a characteristic of strong coupling. The residual  $\gamma_0$  term, although small (0.05 mJ K<sup>-2</sup> g-at.<sup>-1</sup>), is not expected to be an intrinsic property of the A15 phase. It is natural to interpret this term as the contribution of an impurity

phase in the normal state. Since Nb<sub>3</sub>Al is marginally stoichiometric, we admit that this impurity phase is  $\sigma$ -Nb<sub>2</sub>Al. In order to estimate this fraction, the heat capacity of a Nb<sub>0.69</sub>Al<sub>0.31</sub> sample was measured between 2 and 10 K (this composition is about the Nb-rich limit of the  $\sigma$  phase). The data could be fitted within 0.5% rms deviation to the polynomial  $C = \gamma T + \beta_1 T^3 + \beta_2 T^5$ , where,  $\gamma = 2.44$  mJ K<sup>-2</sup> g-at.<sup>-1</sup>,  $\beta_1 = 2.79 \times 10^{-2}$  mJ K<sup>-4</sup> g-at.<sup>-1</sup> [i.e.,  $\Theta(0) = 412$  K], and  $\beta_2 = 3.6 \times 10^{-5}$  mJ K<sup>-6</sup> g-at.<sup>-1</sup>. The absence of any superconducting jump confirms the work of Müller.<sup>6</sup> The parasitic  $\gamma_0$  found both in quenched and annealed Nb<sub>3</sub>Al samples now yields a  $\sigma$ -phase content of 2 at.%. X-ray powder-diffraction patterns were not sensitive enough to detect this amount and the Widmannstätten structure obscures the detection of a second phase in optical micrographs. We note that the  $\gamma$  coefficient of single-phase Nb<sub>3</sub>Al will be 1.6% above that of our samples due to the Nb<sub>2</sub>Al admixture, but this very small correction will not be included in Tables I and II.

The inverse slope of the graph of Fig. 2 is proportional to the third power of the initial Debye temperature  $\Theta(0)$ , which is, in turn, closely related to the velocity of sound.  $\Theta(0)$  is affected by the ordering process, an effect that can be explained by an enhanced screening in the ordered state where the electronic density of states (DOS) at the Fermi level is higher. This effect is confined to the lower part of the phonon spectrum as it is readily apparent from the plot of the effective Debye temperature  $\Theta(T)$  (Fig. 3). Above  $T_c$  the effective  $\Theta$ 's differ by less than 10 K. The behavior just described is in qualitative agreement with the trend found in other A15 compounds.<sup>7</sup> For the series Nb<sub>3</sub>Ir-Nb<sub>3</sub>Pt-Nb<sub>3</sub>Au, the inverse correlation between the

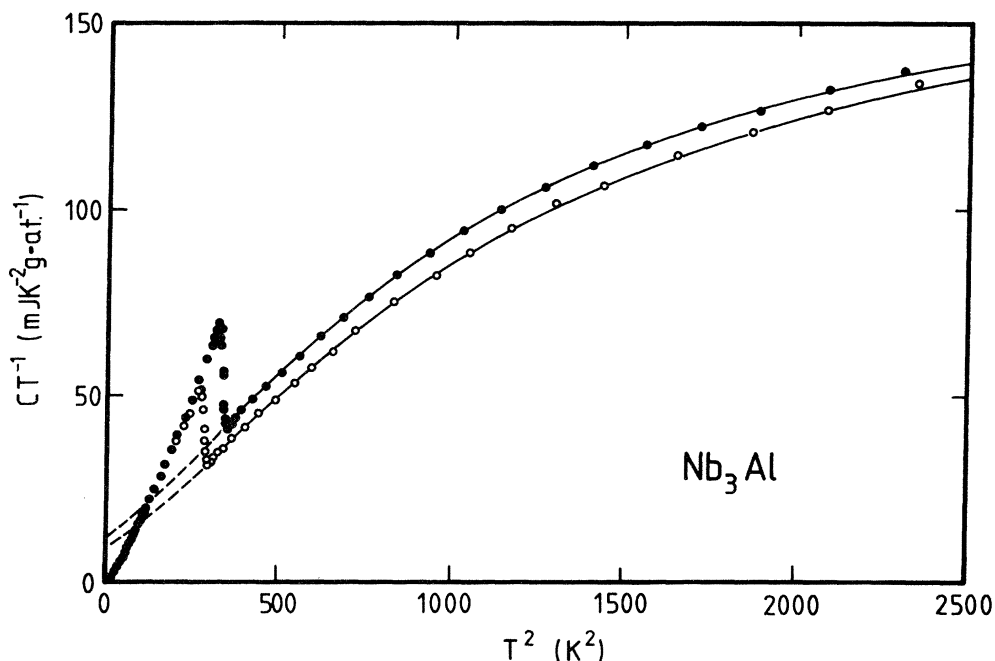


FIG. 1. Specific heat divided by the temperature vs temperature squared in the range 1.3–50 K. Samples: ○—Nb<sub>3</sub>Al quenched, and ●—Nb<sub>3</sub>Al annealed (sample code 255cs). The full line is the fitted normal-state specific heat.

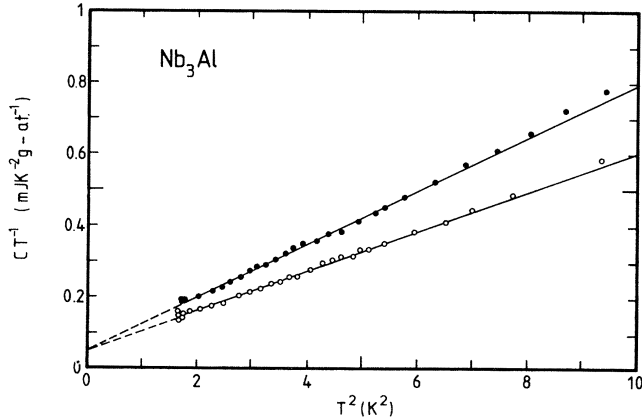


FIG. 2. Specific heat divided by the temperature vs temperature squared in the range 1.3–3 K (superconducting state). Samples: ○—Nb<sub>3</sub>Al quenched, and ●—Nb<sub>3</sub>Al annealed (sample code 255cs).

DOS and  $\Theta(T=0)$  is well established (see Fig. 5 of Ref. 7).

The analysis of the specific-heat curves proceeds as outlined in previous papers.<sup>7,8</sup> We recall that rather than fitting a polynomial curve to extrapolate the normal-state data, we fit a six-parameter model of the phonon spectrum,

$$F(\omega) = \sum_{i=1}^3 D_i F_D(\omega/T_i),$$

where  $F_D(\omega/T_i)$  stands for an elementary Debye spectrum characterized by a partial Debye temperature  $T_i$ , together with an electronic term  $\gamma T$ , to the data between  $T_c$  and 50 K. This procedure is subjected to three constraints: The normal-state entropy should be equal to the superconducting-state entropy at  $T_c$ ; the initial curvature of the phonon spectrum is determined by the initial Debye temperature  $\Theta(0)$ ; the phonon spectrum is normalized to unity (equivalently,  $C \rightarrow 3R$  when  $T \rightarrow \infty$ ). A smaller set of parameters is not able to adequately fit the structure in the specific-heat curve in the entire temperature range. The rms deviation of the fits is close to 1%. The adjusted curves are shown in Fig. 1 and the parameters of the fit are given in Table I.

A new result is the high electronic specific heat found in the ordered sample:  $\gamma = 11.2 \text{ mJ K}^{-2} \text{ g-at.}^{-1}$ . This figure can be compared with the values of 12–14  $\text{mJ K}^{-2} \text{ g-at.}^{-1}$  we find in Nb<sub>3</sub>Sn,<sup>8</sup> and exceeds that of Nb<sub>3</sub>Au<sub>0.7</sub>Pt<sub>0.3</sub>, which is the Nb-based transition-metal A15 phase with the highest  $T_c$  ( $\gamma = 10.1 \text{ mJ K}^{-2} \text{ g-at.}^{-1}$ ,  $T_c = 12.9 \text{ K}$ ). The new  $\gamma$  is substantially higher than generally quoted values for Nb<sub>3</sub>Al (the latter will be reviewed in the next section).

The validity of the extrapolation that determines  $\gamma$  can be visualized in a plot of  $S/T$  vs  $T^2$  where  $S$  is the entropy. Such a plot is similar to the usual  $C/T$  vs  $T^2$ , but gives less weight to the phonon contribution, and contains the entropy condition. If

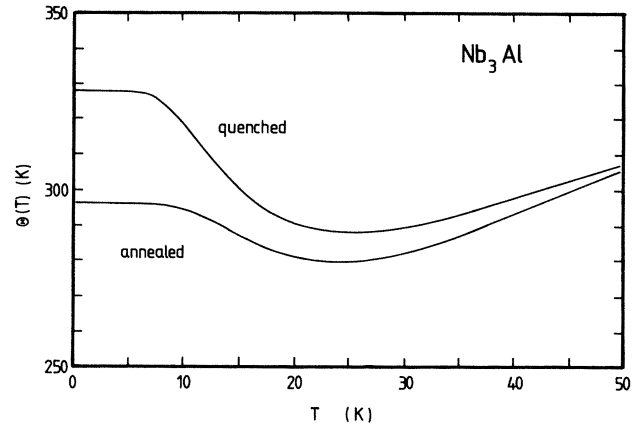


FIG. 3. Effective Debye temperature vs temperature in quenched and annealed Nb<sub>3</sub>Al (sample code 255cs).

$$C/T = \gamma + \beta_1 T^2 + \beta_2 T^4 + \dots,$$

then, using the third law,

$$S/T = \gamma + \frac{1}{3}\beta_1 T^2 + \frac{1}{5}\beta_2 T^4 + \dots$$

A straight-line extrapolation from above  $T_c$  gives a lower limit  $\gamma^- = 10.1 \text{ mJ K}^{-2} \text{ g-at.}^{-1}$ , but too low a value for  $\Theta$ . Restoring correctly the measured  $\Theta(0)$  pushes  $\gamma$  to the above-mentioned value.

The model of the phonon spectrum obtained by the fitting procedure can only be crude (Fig. 4); however, it reproduces the overall weighting of the different parts of the spectrum as measured by inelastic neutron scattering.<sup>9</sup> The results of our “inversion” procedure are qualitatively similar for several samples: Figure 4 includes data on the less homogeneous sample quoted in our earlier work.<sup>8,10</sup>

We are not interested in the detailed features, but rather in integral properties of the spectrum. Some moments are given in Table I; they are defined by

$$\langle \omega^n \rangle = \int \omega^n F(\omega) d\omega.$$

Note that these moments do not rely explicitly on the model for  $F(\omega)$ , as long as this model fits the data correctly, since direct relations such as

$$\int_0^\infty dT \frac{c}{T^3} = (7.212 \dots) \langle \omega^{-2} \rangle,$$

$$\int_0^\infty dT \frac{c}{T^2} = \frac{\pi^2}{3} \langle \omega^{-1} \rangle,$$

$$\int_0^1 dT \frac{c}{T} + \int_1^\infty dT \frac{1-c}{T} = 1 - \langle \ln \omega \rangle,$$

$$\int_0^\infty dT (1-c) = \frac{1}{2} \langle \omega \rangle,$$

where  $c$  is shorthand for  $C(\text{phonon})/3R$ , do exist.<sup>11</sup> The values obtained show again that the phonon softening

TABLE I. Calorimetric data: Results of the fitting procedure. See text for definitions.

Nb <sub>3</sub> Al sample	Quenched	Annealed
$S$ (mJ K <sup>-1</sup> g-at. <sup>-1</sup> )	277	389
at $T_n$ (K)	17.23	18.72
Number of points	114	112
rms deviation ( $T_n - 50$ K)	1.0%	1.1%
$\gamma$ (mJ K <sup>-2</sup> g-at. <sup>-1</sup> )	9.4 <sub>1</sub>	11.2 <sub>4</sub>
$D_1, T_1$ (K)	$-7.50 \times 10^{-3}, 72.4$	$-1.24 \times 10^{-2}, 91.7$
$D_2, T_2$ (K)	0.437, 220	0.444, 209
$D_3, T_3$ (K)	0.571, 429	0.569, 458
$\Theta(T=0)$ (K)	328	296
$\langle \omega^{-2} \rangle^{-1/2}$ (K)	177	171
$\langle \omega^{-1} \rangle^{-1}$ (K)	208	206
$\exp \langle \ln \omega \rangle$ (K)	233	236
$\langle \omega \rangle$ (K)	255	264
$\bar{T}_c$ (K)	16.84	18.45
$\Delta C / \gamma \bar{T}_c$ (BCS theory: 1.43)	2.29	2.35
$\mu_0 H_c(0)$ (T)	0.431	0.523
$-\frac{\bar{T}_c}{H_c(0)} \left[ \frac{\partial H_c}{\partial T} \right]_{T_c}$ (BCS theory: 1.74)	1.99	1.99
$\gamma \bar{T}_c^2 / \mu_0 V H_c^2(0)$ (BCS theory: 2.11)	1.72	1.68
$[D(t)]_{\max}$	+ 1.7%	+ 2.2%

upon annealing is limited to the lowest moments of the phonon spectrum. In particular,  $\langle \omega \rangle / \langle \omega^{-1} \rangle$  does not change significantly.

We now turn to the data given by the specific heat in

the superconducting state. The first one is the transition temperature itself, or rather the distribution of the transition temperatures. In Fig. 5 we show the superconducting volume fraction  $f_s(T)$  computed in the two-fluid model,

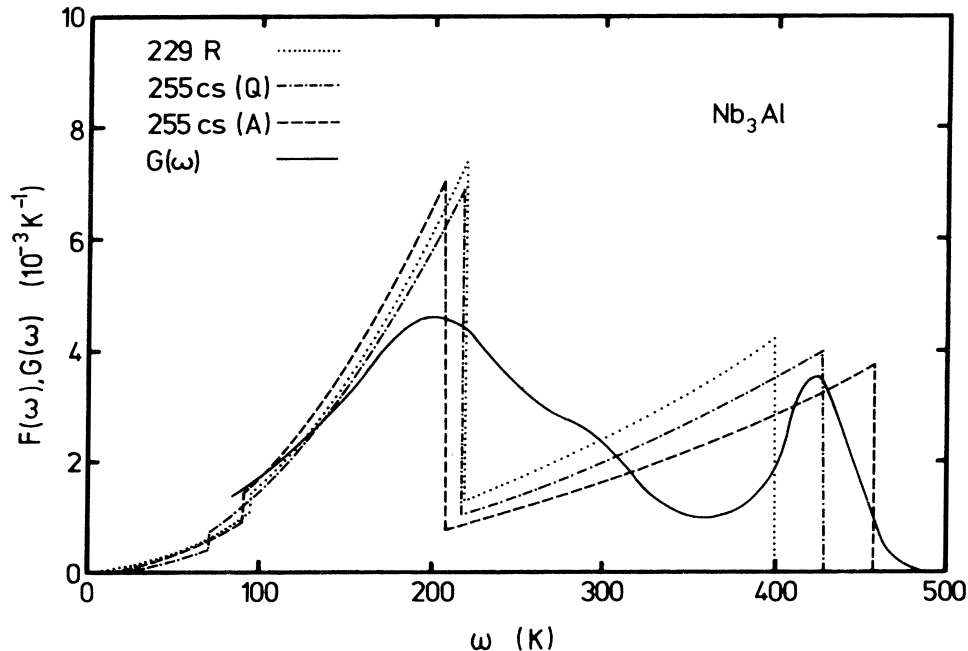


FIG. 4. Full line: generalized phonon spectrum  $G(\omega)$  of Nb<sub>3</sub>Al as determined by Ref. 9. Other lines: fitted models of the phonon spectra in Nb<sub>3</sub>Al (quenched), Nb<sub>3</sub>Al (annealed) (sample code 255cs), and in an unhomogenized "Nb<sub>3</sub>Al" sample (sample code 229R).

$$f_s(T) = \frac{C_s - C_n - 3(S_s - S_n)}{2\gamma T},$$

where  $n$  and  $s$  refer to the normal and superconducting states, and  $S$  is the entropy. The fact that  $f_s(T)$  rises above 1 is not fundamental; it means that the actual specific-heat jump at  $T_c$  is higher than in the two-fluid model—which was chosen for the sake of simplicity. The interesting point is that the new measurements provide a basis on which the  $T_c$  distribution of less homogeneous samples, calculated in the same way, can rely. The example chosen in Fig. 5 is the less homogeneous sample studied in earlier work. Its curve  $f_s(T)$  departs from that of the reference compound at 14 K. The superconducting volume then gradually decreases and vanishes at 18.8 K ( $T_c$  onset). The broadening of  $T_c$  is the signature of a distribution of Al concentrations. Based on published  $T_c$ -versus-composition curves for the same degree of order,<sup>3</sup> we conclude that the composition of the alloy is distributed between  $\approx 21.5$  and  $\approx 24.5$  at. % Al. Turning to the phase diagram, it means that segregation occurred during the cooling in the arc furnace down to a temperature of  $\approx 1300^\circ\text{C}$ .

The specific-heat curves measured near  $T_c$  in the best Nb<sub>3</sub>Ge samples<sup>12</sup> look like those found in the earlier Nb<sub>3</sub>Al work. We suggest that Nb<sub>3</sub>Ge, which is now claimed to be a low- $\gamma$  soft-phonon superconductor, will be only fully understood when samples with a sharp transition will be available. Considering the difficulties in the preparation of this metastable phase, this may remain a challenge for still some more time.

The specific heat of Nb<sub>3</sub>Al in the superconducting state further yields the thermodynamical critical field  $H_c(T)$ ,

the deviation function of the critical field  $D(t)$  and an estimate of the zero-temperature gap.

The variation of  $H_c(0)$  with order reflects the variation of  $\gamma$ . The value in the ordered compound is now equal to that of Nb<sub>3</sub>Sn.<sup>8</sup> This is consistent with the fact that  $\gamma$ ,  $T_c$ , and the coupling strength are similar.

The deviation function

$$D(T/T_c) = [H_c(T)/H_c(0)] - [1 - (T/T_c)^2]$$

reflects the coupling strength (Fig. 6). On a qualitative scale, Nb<sub>3</sub>Al is intermediate between Nb<sub>3</sub>Sn and V<sub>3</sub>Ga. The change after ordering, although of the expected sign, is not very pronounced.

The plot of the reduced electronic specific heat in the superconducting state (Fig. 7) is compared to the curves calculated in the  $\alpha$  model.<sup>13</sup> It seems safe to conclude that  $2\Delta(0)/kT_c$  is comprised between 4.5 and 5. Higher values quoted by Cort *et al.*<sup>14</sup> are implicitly based on the assumption of a constant gap all the way up to  $T_c$ , a condition which is, of course, not fulfilled.

#### IV. SPECIFIC-HEAT DATA FROM OTHER SOURCES

Willens *et al.*<sup>1</sup> measured a sample prepared by a powder metallurgy method. They avoided melting and obtained a sample qualified 95% single phase. A first heat treatment was applied at  $1700^\circ\text{C}$  (homogenization), the resulting  $T_c$  being 17.5 K. After annealing at  $700^\circ\text{C}$ ,  $T_c$  (onset) reached 18.8 K. The values quoted for  $\gamma$  and  $\Theta$  are  $7.95 \text{ mJ K}^{-2} \text{ g-at.}^{-1}$  and 290 K in the lower- $T_c$  sample, and  $7.53 \text{ mJ K}^{-2} \text{ g-at.}^{-1}$  and 290 K in the higher- $T_c$  sample. The authors note that the transition is "not as sharp as is often observed for a well-ordered stoichiometric com-

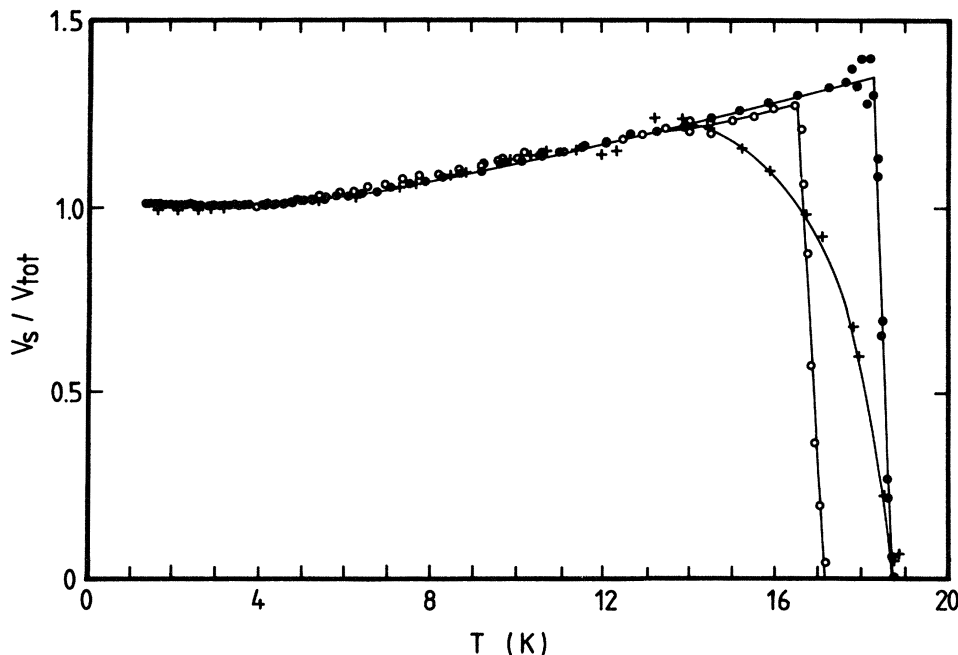


FIG. 5. Ratio of the superconducting volume to the total volume vs temperature. Samples:  $\circ$ —Nb<sub>3</sub>Al quenched,  $\bullet$ —Nb<sub>3</sub>Al annealed (sample code 255cs), and  $+$ —unhomogenized "Nb<sub>3</sub>Al" (sample code 229R).

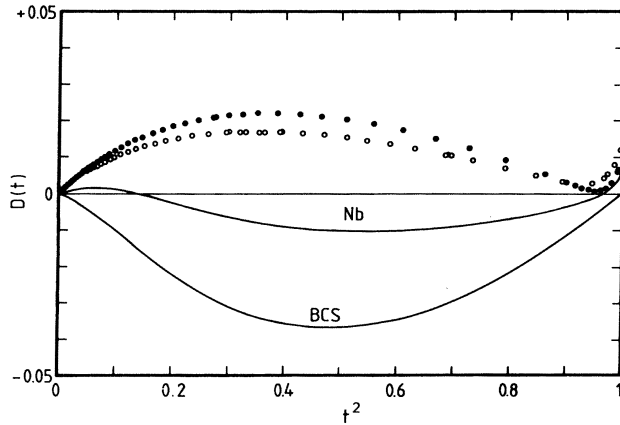


FIG. 6. Deviation function of the thermodynamic critical field vs the reduced temperature squared. Samples:  $\circ$ — $\text{Nb}_3\text{Al}$  quenched, and  $\bullet$ — $\text{Nb}_3\text{Al}$  annealed (sample code 255cs); high-purity niobium and BCS limit are shown for comparison.

pound.” From the phase diagram, we expect that the composition of the  $A15$  phase homogenized at  $1700^\circ\text{C}$  will be  $\text{Nb}_{0.77}\text{Al}_{0.23}$ ; it is not evident, however, that equilibrium relations apply to a sample prepared by powder metallurgy methods. The concentration distribution depends on the cooling rate, which was not specified. The inverse scaling of  $T_c$  and  $\gamma$  denotes extrapolation difficulties.

Knapp *et al.*<sup>15</sup> measured a sample prepared by melting compacted powders in a levitation furnace. The heat treatments were made at  $1550$  and  $600^\circ\text{C}$  (for one week). The sample was qualified 90% single phase. The value quoted for  $\gamma$  is  $7.63 \text{ mJK}^{-2} \text{ g-at.}^{-1}$ . Based on measurements up to room temperature, several moments of the phonon spectrum were given. Again, we note that the equilibrium composition of the  $A15$  phase at  $1550^\circ\text{C}$  is  $\text{Nb}_{0.78}\text{Al}_{0.22}$ . This explains the low values of  $\gamma$  quoted by Knapp *et al.*

Spitzli<sup>16</sup> measured a sample prepared by arc melting that was nominally stoichiometric (Fig. 8). No homogenization was attempted. The specific-heat jump is considerably smeared below  $\approx 17.4 \text{ K}$ ;  $\gamma = 7.9 \text{ mJK}^{-2} \text{ g-at.}^{-1}$ . We measured the same sample after a low-temperature anneal;<sup>10,16</sup> the results have already been discussed above and were similar to those of Willens *et al.*

Cort *et al.*<sup>14</sup> made several measurements as a function of neutron damage. The samples were obtained by arc melting followed by anneals at  $1760$  and  $750^\circ\text{C}$  (for 1 week). The values reported for  $\gamma$  and  $\Theta(0)$  are  $9 \text{ mJK}^{-2} \text{ g-at.}^{-1}$  and  $283 \text{ K}$  in the unirradiated sample. The same remarks apply to this work. The lattice parameter quoted ( $5.186 \text{ \AA}$ ) characterizes an off-stoichiometric composition, close to  $\text{Nb}_{0.77}\text{Al}_{0.23}$ . From the  $C/T$ -vs- $T^2$  plot in the same paper, we see that the specific heat in the superconducting state departs from the linear ( $T^3$ -like) behavior expected in ideal samples near  $T_c$  above  $\approx 16.7 \text{ K}$ , an indication of a distributed  $T_c$ . The maximum value of  $C/T$  just below  $T_c$  found by Cort *et al.*, close to  $58 \text{ mJK}^{-2} \text{ g-at.}^{-1}$ , is nearly equal to that we found in a homogeneous  $\text{Nb}_{0.77}\text{Al}_{0.23}$  sample<sup>3</sup> (Fig. 8), but represents

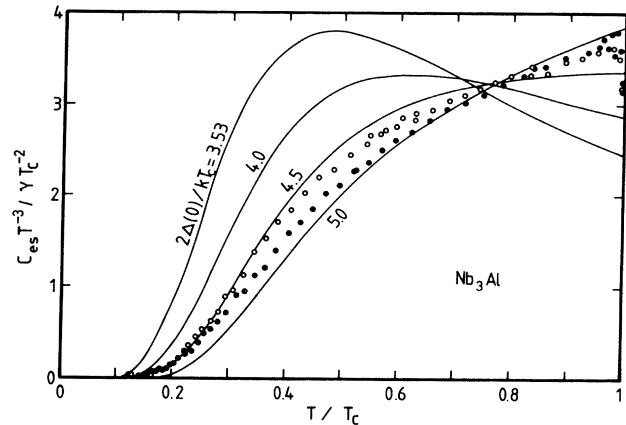


FIG. 7. Reduced electronic specific heat in the superconducting state vs reduced temperature. Full lines: theoretical curves (“ $\alpha$  model”) for various gap ratios. Samples:  $\circ$ — $\text{Nb}_3\text{Al}$  quenched, and  $\bullet$ — $\text{Nb}_3\text{Al}$  annealed (sample code 255cs).

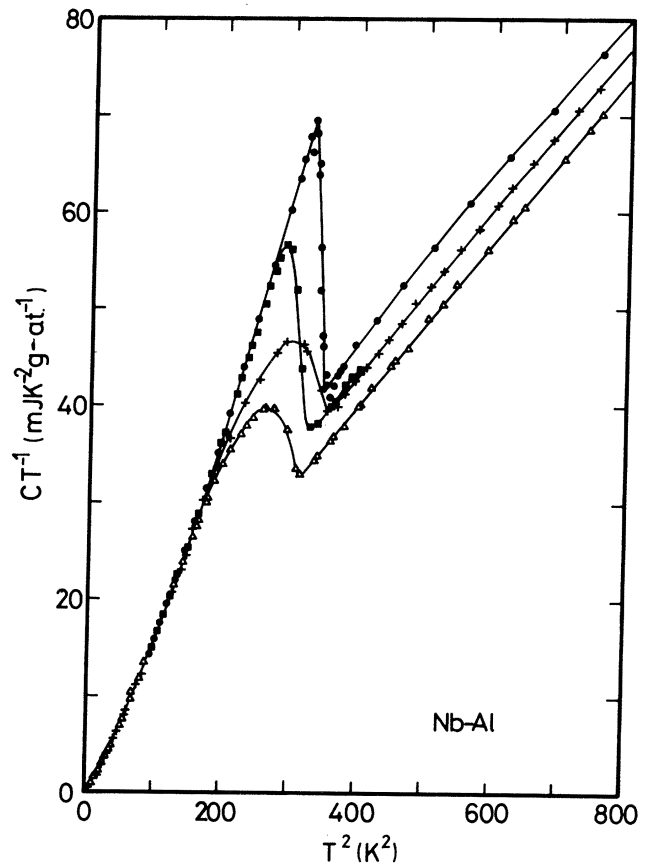


FIG. 8. Specific heat in the vicinity of  $T_c$  divided by the temperature vs temperature squared showing distinctly the importance of the homogenization near  $1940^\circ\text{C}$ . Samples:  $\bullet$ — $\text{Nb}_3\text{Al}$  homogenized, quenched, and annealed (sample code 255cs),  $\blacksquare$ — $\text{Nb}_{0.77}\text{Al}_{0.23}$  homogenized without quenching,  $\triangle$ —“ $\text{Nb}_3\text{Al}$ ” arc melted (sample code 229T), and  $+ -$  “ $\text{Nb}_3\text{Al}$ ”, same sample annealed (sample code 229R).

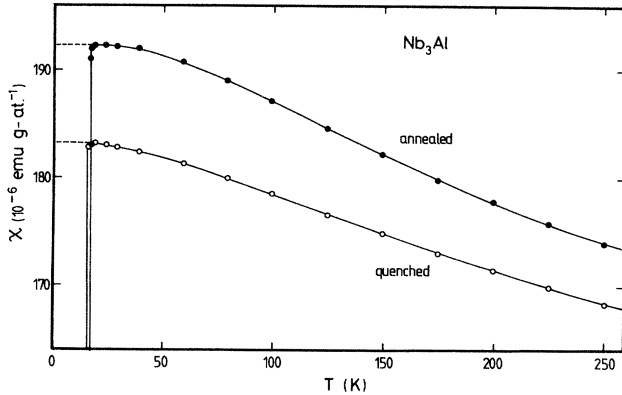


FIG. 9. Magnetic susceptibility vs temperature in the range  $T_c$  to room temperature. Samples:  $\circ$ —Nb<sub>3</sub>Al quenched, and  $\bullet$ —Nb<sub>3</sub>Al annealed (sample code 255cs).  $\chi$  of the annealed sample is  $172.5 \times 10^{-6}$  emu g-at.<sup>-1</sup> at 293 K.

only 83% of the maximum in the ordered Nb<sub>3</sub>Al sample reported here. Together with the fact that the specific-heat measurements as a function of irradiation were taken on different samples in Cort's work, these remarks explain why our conclusions concerning the phonon softening versus the variation of the DOS in ordering processes will be at variance with those of Cort *et al.*

### V. SUSCEPTIBILITY

The susceptibility measurements in the temperature range of 250 K down to the superconducting transition temperature and in magnetic fields of 0.5 to 2 T were performed with a superconducting quantum-interference device (SQUID) susceptometer<sup>17</sup> on the same samples used to collect the specific-heat data. The absolute accuracy is about 1%, while the relative accuracy between different measurements in the same operating conditions is estimated to be better than 0.5%.

The temperature dependence of the magnetic susceptibility of Nb<sub>3</sub>Al in the normal state is presented in Fig. 9. Corrections for the field dependence of the susceptibility were made and indicate less than 10 at. ppm of ferromagnetic impurities in the samples. The amount of paramagnetic impurities is conservatively estimated to be of the same order of magnitude because, within the experimental accuracy, no such contribution can be detected. No correction was applied for the small susceptibility of the Nb<sub>2</sub>Al impurity phase.<sup>18</sup>

The magnetic susceptibility of Nb<sub>3</sub>Al increases continuously upon lowering the temperature and tends to saturate below about 20 K. For the annealed sample, we find a value of  $192 \times 10^{-6}$  emu g-at.<sup>-1</sup> at the lowest temperatures and a maximum slope  $d\chi/dT$  of about  $-9.5 \times 10^{-8}$  emu g-at.<sup>-1</sup> K<sup>-1</sup> in the intermediate range. Both figures are somewhat higher than those previously reported.<sup>1,19,20</sup> The curve of the quenched Nb<sub>3</sub>Al sample is shifted downwards with a low-temperature susceptibility of  $183 \times 10^{-6}$  emu g-at.<sup>-1</sup> and a maximum slope of about  $-7.5 \times 10^{-8}$  emu g-at.<sup>-1</sup> K<sup>-1</sup>. As both samples have exactly the same

stoichiometry, the shift of about 5% in the absolute value of the susceptibility between the two samples is attributed to ordering effects on the atomic sites.

### VI. DISCUSSION

The central problem is to explain the favorable superconducting properties of Nb<sub>3</sub>Al in relation to similar compounds. In order to get a deeper insight, some information on the Eliashberg function  $\alpha^2F(\omega)$  is required.  $\alpha^2F$  is available from tunneling data,<sup>21</sup> on slightly off-stoichiometric films, but we feel that additional information, representative of the bulk material rather than the surface, is useful.

It is well known that the function  $\alpha^2F(\omega)$  resembles the phonon spectrum, with more weight added to low-energy modes. From similar studies in Nb<sub>3</sub>Sn (Ref. 8), Nb, and V,<sup>22</sup> we have found that for the present purpose, the weighting can be adequately approximated by an empirical function  $\alpha^2(\omega)$  such that

$$\frac{d \ln \alpha^2(\omega)}{d \ln \omega} = s,$$

where  $s$  is close to  $-0.5$ . (We could just as well choose two values of  $\alpha^2$  differing by a constant factor for the acoustical and the optical modes; essentially, we want to introduce a minimum of adjustable parameters.) With the choice of  $s = -0.5$ , the moments of  $\alpha^2F(\omega)/\omega$  defined by

$$\ln(\omega_{\log}) = \frac{\int d\omega (\ln \omega \alpha^2 F / \omega)}{\int d\omega (\alpha^2 F / \omega)},$$

$$(\bar{\omega}_n)^n = \frac{\int d\omega (\omega^n \alpha^2 F / \omega)}{\int d\omega (\alpha^2 F / \omega)}$$

agree with those determined by inversion of tunneling characteristics in Nb<sub>3</sub>Sn, Nb, and V.

Using the spectra  $F(\omega)$  fitted to the specific-heat curves and this approximation for  $\alpha^2$ , the moments defined above are calculated and introduced into the full interpolation equation of Allen and Dynes,<sup>23</sup>  $\mu^*$  is set to 0.13. We obtain the electron-phonon coupling parameter  $\lambda$ , the average value of  $\alpha^2(\omega)$ , the average matrix element of the electron-phonon coupling  $\langle I^2 \rangle$ , the bare DOS  $N(0)$  and the electronic parameter  $\eta = N(0) \langle I^2 \rangle$ . These figures are given in Table II; the effect of different choices for  $s$  is also indicated.

The moments of  $\alpha^2F(\omega)/\omega$  we obtain empirically in bulk stoichiometric samples are systematically higher than those determined by inversion of tunneling characteristics. The values  $\omega_{\log} = 130(110)$  K,  $\bar{\omega}_1 = 154(132)$  K, and  $\bar{\omega}_2 = 174(156)$  K have been reported in two off-stoichiometric films with  $T_c = 14.0(16.4)$  K.<sup>21</sup> On the other hand, the DOS we determine is equal to the average of the published band-structure calculations [ $N(0) = 0.84$ ,<sup>24</sup> 0.91,<sup>25</sup> and 0.97 states eV<sup>-1</sup> atom<sup>-1</sup> (1-spin)<sup>-1</sup> (Ref. 26)]. A further support to these calculations, which generally place the Fermi level close to a peak of the DOS, is the noticeable variation of the susceptibility versus tem-

TABLE II. Microscopic parameters obtained with the use of the model  $\alpha^2F(\omega) = \text{const}\omega^sF(\omega)$ . The uncertainty margins correspond to the limits  $s=0$  (upper number) and  $s=-1$  (lower number). See text for definitions.

Nb <sub>3</sub> Al sample	Quenched	Annealed
$\omega_{\log}$ (K)	$153^{+29}_{-39}$	$145^{+33}_{-42}$
$\bar{\omega}_1$ (K)	$181^{+26}_{-31}$	$176^{+30}_{-34}$
$\bar{\omega}_2$ (K)	$205^{+25}_{-29}$	$204^{+30}_{-33}$
$\lambda$	$1.43^{+0.17}_{-0.41}$	$1.62^{+0.24}_{-0.60}$
$\bar{\alpha}^2$ (K)	$130^{+1}_{-7}$	$142^{+0}_{-15}$
$\eta$ (eV Å <sup>-2</sup> )	$8.2^{+0.9}_{-0.4}$	$9.1^{+1.1}_{-0.3}$
$\langle I^2 \rangle$ (eV <sup>2</sup> Å <sup>-2</sup> )	$10.0^{+0.3}_{-1.0}$	$10.0^{+0.1}_{-1.9}$
$M\bar{\omega}_2^2$ (eV Å <sup>-2</sup> )	$5.7^{+1.5}_{-1.5}$	$5.6^{+1.8}_{-1.6}$
$N(0)$ [eV <sup>-1</sup> atom <sup>-1</sup> (1-spin) <sup>-1</sup> ]	$0.82^{+0.06}_{-0.12}$	$0.91^{+0.09}_{-0.17}$
$N(0)$ [Ry <sup>-1</sup> (unit cell) <sup>-1</sup> (2-spin) <sup>-1</sup> ]	$179^{+13}_{-26}$	$198^{+20}_{-37}$

perature. Finally, the value found for  $\langle I^2 \rangle$  is common to a large set of Nb-based *A15* compounds.<sup>8</sup>

The variation of these microscopic parameters when the atomic long-range order is modified is more informative in view of the mechanism of superconductivity than the values themselves. In Table III we list the relative increments of the “ingredients” that make up  $T_c$ . Qualitatively similar results have been tabulated for Nb<sub>3</sub>Pt, Nb<sub>3</sub>Pt<sub>0.6</sub>Au<sub>0.4</sub>, Nb<sub>3</sub>Pt<sub>0.3</sub>Au<sub>0.7</sub>, V<sub>3</sub>Au, and V<sub>3</sub>Ga.<sup>8</sup>

As one keeps in mind the relation

$$\lambda = N(0)\langle I^2 \rangle (M\bar{\omega}_2^2)^{-1},$$

it is interesting to note that some qualitative conclusions *do not depend on the choice of  $s$* . These conclusions are the following.

(i) The variation of the denominator  $M\bar{\omega}_2^2$ , a phonon quantity, is much smaller than the variation of the numerator  $\eta$ , which is essentially electronic.

(ii) The softening of the very-low-frequency modes, represented by  $\omega_{\log}$ , has a detrimental effect on  $T_c$ . This is immediately apparent in Allen and Dyne’s expression, while in the formalism of the functional derivatives  $\delta T_c / \delta \alpha^2 F(\omega)$ , it takes away modes in a region where they have a peak efficiency on  $T_c$  ( $\approx 2\pi T_c$ ) and puts them in a less effective region.

The question of the origin of the variation of the numerator  $\eta$  depends more on the weighting function  $\alpha^2(\omega)$ . Considering the results obtained with  $s = -0.5$  or 0, we conclude that the key factor is the DOS. The results obtained with  $s = -1$ , although they bring the moments of  $\alpha^2 F(\omega)/\omega$  in better agreement with tunneling, yield the unphysical result that  $\langle I^2 \rangle$  increases as  $N(0)$  increases.

Concerning the controversy about the importance of lattice softening versus large  $N(0)$  to explain the high  $T_c$  of Nb<sub>3</sub>Al, we would like to comment on the usual interpretation of tunneling results. Kwo and Geballe<sup>21</sup> observe an enhancement of  $\alpha^2 F(\omega)$ , mainly below the acoustic peak, when  $T_c$  increases as a function of composition (which is an effect similar, but not identical, to the variation of long-range order at constant composition reported here). They conclude that “the important contribution of lattice softening to the high  $T_c$  in metastable Nb<sub>3</sub>Al has

been well established rather than a large  $N(0)$  conventionally used to explain the high- $T_c$  and normal-state properties of V<sub>3</sub>Si and Nb<sub>3</sub>Sn.” This point of view is expressed in several other articles.<sup>12,14,27,28</sup> They base this assertion on the measured  $\alpha^2 F(\omega)$  curves in two samples with  $T_c = 14$  and 16.4 K, and on earlier lower  $\gamma$  values. The latter argument should now be reconsidered, but we should like to point out further that the observed enhancement of  $\alpha^2 F(\omega)$  does not decide unambiguously in favor of the importance of phonon softening. Strictly speaking, an increase of  $\alpha^2 F$  may be the superposition of two effects: the shift of phonons to lower frequencies in a region of the spectrum where  $dF(\omega)/d\omega$  is positive on one hand (this “true” softening can be measured by neutron scattering for selected modes, or by specific heat for an average value), and an increase of  $\alpha^2(\omega)$  on the other hand. Clearly, this second effect contains a contribution of the DOS since in fact the first moment of  $\alpha^2 F(\omega)$  is an electronic quantity,

$$2M \int d\omega \omega \alpha^2 F(\omega) = N(0)\langle I^2 \rangle.$$

It is certain that this integral of the Eliashberg function as measured by tunneling increases with  $T_c$  both in the Nb<sub>3</sub>Al and in the Nb<sub>3</sub>Ge systems. It follows that the tunneling results do not contradict our interpretation.

TABLE III. Relative increments of the physical parameters that determine  $\lambda$  and  $T_c$  during the annealing process. The figures are calculated with  $s = -0.5$  (see text); the cases  $s = 0$  and  $s = 1$  are also listed.

	Nb <sub>3</sub> Al		
	$s = -0.5$	$s = 0$	$s = 1$
$\Delta \bar{T}_c / \bar{T}_c$	+ 10%	+ 10%	+ 21%
$\Delta \lambda / \lambda$	+ 13%	+ 10%	+ 21%
$\Delta \eta / \eta$	+ 11%	+ 12%	+ 13%
$-\Delta \bar{\omega}_2^2 / \bar{\omega}_2^2$	+ 1%	+ 2%	+ 4%
$\Delta N(0) / N(0)$	+ 11%	+ 14%	+ 5%
$\Delta \omega_{\log} / \omega_{\log}$	- 6%	- 2%	- 10%



Our last point concerns the assessment of the presence—or absence—of spin fluctuations in Nb<sub>3</sub>Al. This question has been raised by several authors, mainly in Ref. 29; V-based A15 compounds with a high DOS seem to be candidates.

For a quantitative test we must extract the Pauli term from the total susceptibility. Considering the two samples studied in this work, which differ only by their long-range order parameter, we admit that the difference of the susceptibilities is entirely due to the spin term. It follows that

$$\Delta\chi = 2\mu_B^2 [N^+(1-\mu^+)^{-1} - N^-(1-\mu^-)^{-1}],$$

where the superscripts  $\pm$  stand for the annealed and for the quenched state.  $(1-\mu)^{-1}$  is the Stoner factor  $S$ ; we admit as a second equation that  $\mu$  is proportional to  $N(0)$ . Solving for  $\mu$ , we find  $\mu^+ = 0.22$ ,  $\mu^- = 0.19$ , or  $\chi - \chi(\text{Pauli}) = 118 \times 10^{-6}$  emu g-at.<sup>-1</sup> [i.e., essentially  $\chi(\text{orbital})$ ];  $\chi^+(\text{Pauli}, T=0) = 75 \times 10^{-6}$  and  $\chi^-(\text{Pauli}, T=0) = 66 \times 10^{-6}$  emu g-at.<sup>-1</sup>. Now the formal parameter of spin fluctuation  $\lambda_{\text{sf}}$  can be estimated,<sup>29</sup>

$$\lambda_{\text{sf}} = 4.5(1-S^{-1}) \ln[1 + \bar{p}_1^2(S-1)/12].$$

Taking  $\bar{p}_1 = 0.6$  as a first approximation, we find  $\lambda_{\text{sf}} \approx 10^{-2}$ . This value is 2 orders of magnitude below the electron-phonon mass-enhancement factor, and even 1 order of magnitude below the screened Coulomb interaction  $\mu^*$ . The estimate justifies *a posteriori* the fact that we have neglected spin fluctuations in the analysis of the Nb<sub>3</sub>Al data.

Let us emphasize that the above conclusion does not depend critically on the assumption that  $\mu \propto N(0)$ . For a *small* variation of  $\chi(\text{Pauli})$  and  $\gamma$ , and in the absence of any correlation effects, we can also write

$$\delta\chi(\text{Pauli}) = \frac{3\mu_B^2}{\pi^2 k_B^2} \frac{\delta\gamma}{1+\lambda},$$

where the symbols have their usual meaning. With the

data given above, one expects  $\delta\chi(\text{Pauli}) = 10 \times 10^{-6}$  emu g-at.<sup>-1</sup>, whereas the measured variation is  $9 \times 10^{-6}$  emu g-at.<sup>-1</sup>. This simple estimate also confirms that a substantial Stoner factor is unlikely.

## VII. CONCLUSIONS

Measurements on homogeneous and nearly stoichiometric Nb<sub>3</sub>Al samples show that the  $\gamma$  coefficient of the A15 phase is close to 11.4 mJ K<sup>-2</sup> g-at.<sup>-1</sup>, including a small correction for the second phase present in the sample. This value is 25–50% above the values quoted in the literature. The difference is explained by the metallurgical state, i.e., only a fraction of a low- $\gamma$  sample is actually superconducting just below the onset transition temperature. This resolves the apparent contradiction between a high  $T_c$  and a low DOS.

The increase of  $T_c$  versus long-range order is accompanied by a substantial increase of  $\gamma$ , and a phonon softening restricted to the low-frequency part of the spectrum, which is not believed to be very effective in raising  $T_c$ . As it was observed in our previous studies of ordering effects in V<sub>3</sub>Au, V<sub>3</sub>Ga, Nb<sub>3</sub>Pt, and Nb<sub>3</sub>Au<sub>1-x</sub>Pt<sub>x</sub>,<sup>8</sup> and in agreement with theoretical models,<sup>30</sup> the key parameter seems to be the DOS at the Fermi level.

The magnetic susceptibility measurements support the idea that some structure exists in the DOS not far from the Fermi level. This suggests lifetime broadening as a possible physical mechanism to explain the variation of  $T_c$  with the order parameter. The orbital part of the susceptibility determined here is quite comparable to that of niobium; further the spin susceptibility is only weakly exchange enhanced. The latter fact excludes the hypothesis that spin-fluctuation effects might limit the superconducting potential of Nb<sub>3</sub>Al.

## ACKNOWLEDGMENTS

This work was supported by the Fonds National Suisse de la Recherche Scientifique.

<sup>1</sup>R. H. Willens, T. H. Geballe, A. C. Gossard, J. P. Maita, A. Menth, G. W. Hull, Jr., and R. R. Soden, *Solid State Commun.* **7**, 837 (1969).

<sup>2</sup>J.-L. Jorda, R. Flükiger, and J. Muller, *J. Less-Common Met.* **75**, 227 (1980).

<sup>3</sup>R. Flükiger, J.-L. Jorda, A. Junod, and P. Fischer, *Appl. Phys. Commun.* **1**, 9 (1981).

<sup>4</sup>G. T. Furukawa, W. G. Saba, M. L. Reilly, *Natl. Bur. Stand. Ref. Data Ser. (U.S.A.)*, No. 18, 1 (1968).

<sup>5</sup>Wakefield Engineering, Inc (Wakefield, Mass.) Type 120 thermal joint compound. The heat capacity is given in B. Lachal, Ph.D. thesis No. 2074, University of Geneva, 1983, p. 29.

<sup>6</sup>A. Müller, *Z. Naturforsch.* **28b**, 472 (1973).

<sup>7</sup>A. Junod, D. Bichsel, and J. Muller, *Helv. Phys. Acta* **52**, 580 (1979).

<sup>8</sup>A. Junod, T. Jarlborg, and J. Muller, *Phys. Rev. B* **27**, 1568 (1983). The coefficient  $\gamma$  of Nb<sub>3</sub>Sn quoted therein [12–14 mJ K<sup>-1</sup> g-at.<sup>-1</sup>] is presently a subject of controversy. Stewart, Cort, and Webb [*Phys. Rev. B* **24**, 3841 (1981)] re-

port  $\gamma = 8.8$  mJ K<sup>-2</sup> g-at.<sup>-1</sup>, based on the extrapolation of normal-state measurements between 8 and 10 K at 18 T (there is an upturn below 8 K). New measurements [G. Stewart (private communication)] indicate a slightly higher  $\gamma$  in the same conditions, but a puzzling fact is that the measurements of  $\gamma^0(H)$  in the *mixed* state near  $T=0$  extrapolate to a much higher  $\gamma$  (above the values we quote in polycrystalline samples). Such effects may be related to *very* fine structures in the DOS with a width of order  $k_B T_c$  or  $\mu_B H_{c2}$ , conceivable only in highest-purity single crystals. In this case normal-state data should be significantly perturbed by an applied field of the same order of magnitude. The value we quote can be considered as an averaged-out  $\gamma$  (it satisfies the entropy condition at  $T_c$ ) in the absence of any field-induced shift of the Fermi level.

<sup>9</sup>For example,  $\langle \omega^2 \rangle^{1/2} \approx 273$  K (neutron scattering) and  $\langle \omega^2 \rangle^{1/2} \approx 275$ –288 K (specific heat). B. P. Schweiss, B. Renker, E. Schneider, and W. Reichardt, in *Superconductivity in d- and f-Band Metals*, edited by D. H. Douglass (Plenum, New York, 1976) p. 189.

- <sup>10</sup>A. Junod, J.-L. Staudenmann, J. Muller, and P. Spitzli, *J. Low Temp. Phys.* **5**, 25 (1971).
- <sup>11</sup>A. Junod, *Solid State Commun.* **33**, 55 (1980).
- <sup>12</sup>G. R. Stewart, L. R. Newkirk, and F. A. Valencia, *Solid State Commun.* **26**, 417 (1978).
- <sup>13</sup>H. Padamsee, J. E. Neighbor, and C. A. Shiffman, *J. Low Temp. Phys.* **12**, 387 (1973).
- <sup>14</sup>B. Cort, G. R. Stewart, C. L. Snead, Jr., A. R. Sweedler, and S. Moehlecke, *Phys. Rev. B* **24**, 3794 (1981); *J. Low Temp. Phys.* **51**, 179 (1983).
- <sup>15</sup>G. S. Knapp, S. D. Bader, and Z. Fisk, *Phys. Rev. B* **13**, 3783 (1976).
- <sup>16</sup>P. Spitzli, Ph. D. thesis No. 1541, University of Geneva, 1970; *Phys. Kondens. Mater.* **13**, 22 (1971).
- <sup>17</sup>M. Pelizzone and A. Treyvaud, *Appl. Phys.* **24**, 375 (1981).
- <sup>18</sup>W. Leyarovski, L. Leyarovska, E. Krasnopyorov, L. Kokot, R. Horyń, and T. Mydlarz, *Z. Phys. B* **27**, 57 (1977).
- <sup>19</sup>B. N. Kodess, *Solid State Commun.* **13**, 527 (1973).
- <sup>20</sup>V. F. Shamray and A. M. Postnikov *Izv. Akad. Nauk SSSR Met.*, No. 3, 208 (1977).
- <sup>21</sup>J. Kwo and T. H. Geballe, *Phys. Rev. B* **23**, 3230 (1981).
- <sup>22</sup>A. Junod (unpublished). In Nb, we find (for  $s = -0.5$ )  $\omega_{\log} = 133$  K,  $\bar{\omega}_1 = 162$  K, and  $\bar{\omega}_2 = 180$  K. In V, we find  $\omega_{\log} = 192$ ,  $\bar{\omega}_1 = 222$  K, and  $\bar{\omega}_2 = 242$  K. In Nb<sub>3</sub>Sn, we find  $\omega_{\log} = 125$ ,  $\bar{\omega}_1 = 155$  K, and  $\bar{\omega}_2 = 176$  K.
- <sup>23</sup>P. B. Allen and R. C. Dynes, *Phys. Rev. B* **12**, 905 (1975).
- <sup>24</sup>T. Jarlborg, *J. Phys. F* **9**, 283 (1979).
- <sup>25</sup>B. M. Klein, L. L. Boyer, D. A. Papaconstantopoulos, and L. F. Mattheiss, *Phys. Rev. B* **18**, 6411 (1978).
- <sup>26</sup>W. E. Pickett, K. M. Ho, and M. L. Cohen, *Phys. Rev. B* **19**, 1734 (1979).
- <sup>27</sup>T. H. Geballe, in *Proceedings of the Applied Superconductivity Conference, Knoxville, Tennessee, 1982* (in press).
- <sup>28</sup>J. Kwo and T. H. Geballe, *Physica* **109&110 B**, 1665 (1982).
- <sup>29</sup>T. P. Orlando and M. R. Beasley, *Phys. Rev. Lett.* **46**, 1598 (1981). A missing  $\bar{\Gamma}$  prefactor in Eq. (7) is restored.
- <sup>30</sup>C. M. Varma and R. C. Dynes, in *Superconductivity in d- and f-Band Metals*, Ref. 9, p. 507.